Experiment 1: Rotational Symmetry and Layered Geometric Organization in Water Cymatics Elicited by Traditional Chakra Bīja Mantras

Analytical Record and Publication-Style Draft

Nikhel Kumar Mahajan (Sattyananda)
Nāda Yoga Foundation / Audio Ashram
September 2026

STATUS: Exploratory analytical record / preprint-style working draft. Not peer reviewed.

This document records the complete first-stage analysis of a controlled water-cymatics sequence using the traditional chakra bīja sounds LAM, VAM, RAM, YAM, HAM, and OM, together with a separate layered-OM Ājñā probe. It is written to preserve the experimental observations, quantitative image-analysis results, candidate frames, interpretive parallels, negative findings, and methodological limitations before subsequent replication or hypothesis refinement.

Abstract

Traditional tantric descriptions of the six principal chakras preserve a structured relationship between bīja syllables, lotus petal counts, and internal geometric motifs. This exploratory experiment asked whether water cymatics driven by traditional chakra bīja recordings produce reproducible rotational organizations that show measurable structural parallels with those numerical and geometric descriptions. A single cymatic apparatus was maintained under unchanged physical conditions while LAM, VAM, RAM, YAM, HAM, and OM were played repeatedly in longer source recordings; representative excerpts were later assembled into a 67.0 s analytical sequence. A separate 9.92 s Ājñā probe combined an OM recording with an octave-lowered copy of itself. Video frames were analysed by polar sampling around the cymatic centre followed by angular Fourier decomposition across multiple radii, allowing rotational orders to be localized by time and radial layer rather than inferred from visual resemblance alone.

Whole-section analysis showed strong expected-order correspondence for LAM/4 and selective higher-order correspondence for HAM/16, while VAM/6 was transient, RAM/10 and YAM/12 were weak when averaged globally, and unmodified OM did not reduce to a single low-order symmetry. Multi-radius analysis materially changed this picture. RAM contained repeated local 3-fold and dominant 6-fold organization together with a distinct transient 10-fold radial layer; YAM contained intervals in which strong 6-fold organization occurred at an inner/middle radius while 12-fold order became locally dominant at a more external radius; HAM exhibited an 8-fold parent structure with 16-fold finer subdivision; and the layered-OM Ājñā probe showed persistent central 2-fold organization. The final unmodified OM/Sahasrāra observation was characterized instead by dense radial multiplicity and subdivision, with a persistent 4/8/16/24 hierarchy, approximately eleven materially expressed rotational orders on average, and exceptionally strong empirical repeatability across repeated presentations of the same OM stimulus. The findings support a hypothesis that relevant numerical correspondences, where present, may be expressed at different spatial scales within a layered cymatic field rather than as literal outer 'petal' counts.

These data do not establish that chakra structures are physical anatomical entities, that traditional diagrams encode cymatic predictions, or that a given bīja uniquely generates its associated traditional number. The Sahasrāra comparison likewise does not interpret 'one thousand petals' as a literal k=1000 cymatic prediction; it operationalizes the traditional motif conservatively as extreme radial multiplicity and subdivision. The experiment is best interpreted as a hypothesis-generating study of acoustic-visual structure in a fixed fluid-vibration system, with several nontrivial correspondences that merit blinded replication, full-run analysis, acoustic characterization, and independent apparatus validation.

Keywords

cymatics; bīja mantra; chakra; rotational symmetry; angular Fourier analysis; standing-wave pattern; water vibration; Sanskrit phonetics; Nāda Yoga; exploratory image analysis

1. Background and research question

Cymatics is used here in its physically grounded sense: the visualization of vibration-induced spatial organization in a material medium. Classical Chladni and Faraday observations established that driven mechanical systems can form highly ordered nodal and surface-wave structures, and modern studies continue to use vibration-induced patterns as readouts of resonant and standing-wave behaviour. In liquid systems, the observed geometry depends on interacting parameters including drive frequency and amplitude, fluid volume and viscosity, container geometry, boundary conditions, and fluid-structure coupling.

The traditional comparison in this experiment comes from the Ṣaṭ-Cakra-Nirūpaṇa as transmitted in Arthur Avalon's (Sir John Woodroffe's) The Serpent Power. In that scheme the six principal centres are described using both sound and geometry: Mūlādhāra is a four-petalled lotus with an earth mandala described as square; Svādhiṣṭhāna has six petals and a half-moon/water region; Maṇipūra has ten petals and a triangular fire mandala; Anāhata has twelve petals and a six-cornered mandala; Viśuddha has sixteen petals and a round ākāśa mandala; and Ājñā is a two-petalled lotus with OṂ/Pranava in its pericarp. The present work does not assume that these motifs are scientific diagrams. They are treated as predefined historical structures against which measured cymatic symmetry can be compared.

Primary research question

Do traditional chakra bīja stimuli, when coupled into the same water-cymatics apparatus under unchanged recording conditions, generate measurable rotational organizations that show structural correspondences with the numerical and geometric features preserved in the traditional chakra model?

Secondary questions

- Are expected rotational orders visible only as whole-field forms, or can they occur at distinct radial layers within the same cymatic image?
- Are any expected orders selectively enriched in their associated bīja section relative to other bījas?
- Do traditional parent geometries (for example triangular / sixfold relationships) help explain apparently 'mismatched' dominant orders?
- Does a deliberately octave-layered OM stimulus produce a stronger twofold organization relevant to the traditional two-petalled Ājñā comparison?
- Which apparent correspondences survive conservative treatment of confounds such as the circular bowl boundary and harmonic relationships between rotational orders?

2. Traditional comparator used for Experiment 1

Table 1. Historical comparator and a priori structural comparisons used in this analysis.

Centre	Bīja	Petals	Traditional geometric motif	Predefined analytical comparison
Mūlādhāra	LAM	4	Square earth mandala	Fourfold organization
Svādhiṣṭhāna	VAM	6	Half-moon / water region	Sixfold + curved/annular organization
Maṇipūra	RAM	10	Triangular fire mandala	3-fold parent / 6-fold harmonic + 10-fold radial order
Anāhata	YAM	12	Six-cornered mandala	Nested 6-fold + 12-fold organization
Viśuddha	HAM	16	Round ākāśa mandala	16-fold order; circle treated as confounded by bowl
Ājñā	OM	2	Two petals; OṂ/Pranava in pericarp	Central 2-fold organization

Centre	Bīja	Petals	Traditional geometric motif	Predefined analytical comparison
Sahasrāra	OM	1000 / innumerable	Thousand-petalled lotus	Radial multiplicity, subdivision, high-order coexistence

3. Experimental design and source material

3.1 Apparatus constancy

According to the experimenter, the source material was recorded as longer repeated runs rather than as isolated single clips. Each bīja was repeated several times while the physical system remained unchanged. The same bowl, water volume, transducer, camera position, lighting, gain, audio file for the relevant bīja, and playback level were retained throughout the recording session. The excerpts analysed here were subsequently cut from those longer runs and arranged into a sequence for comparison. This is methodologically important because the visual differences between bīja sections were not introduced by deliberate changes in apparatus configuration between clips.

However, the present analytical record quantitatively evaluates the supplied edited excerpts, not the complete uncut repeated runs. The experimenter's observation that the longer runs repeatedly returned to the same characteristic patterns is therefore recorded as an experimental observation to be formally quantified in a subsequent repeatability analysis.

3.2 Primary edited sequence

Table 2. Primary edited sequence metadata.

Parameter	Value
Video	chakra-test.mp4
Duration	67.000 s
Video stream	H.264, 1080 × 1920, 25 fps
Audio stream	AAC, stereo, 48 kHz
Cymatic centre used for analysis	approximately x=525, y=835 px
Primary radial sampling range	approximately 70–320 px (analysis-dependent)

Table 3. Segment boundaries derived from audio minima in the edited sequence.

Segment	Start (s)	End (s)	Duration (s)
LAM	0.0000	8.7863	8.7863
VAM	8.7863	17.9480	9.1617
RAM	17.9480	27.6914	9.7434
YAM	27.6914	36.9186	9.2272
HAM	36.9186	46.8595	9.9409

Segment	Start (s)	End (s)	Duration (s)
OM1	46.8595	56.8234	9.9639
OM2	56.8234	67.0000	10.1766

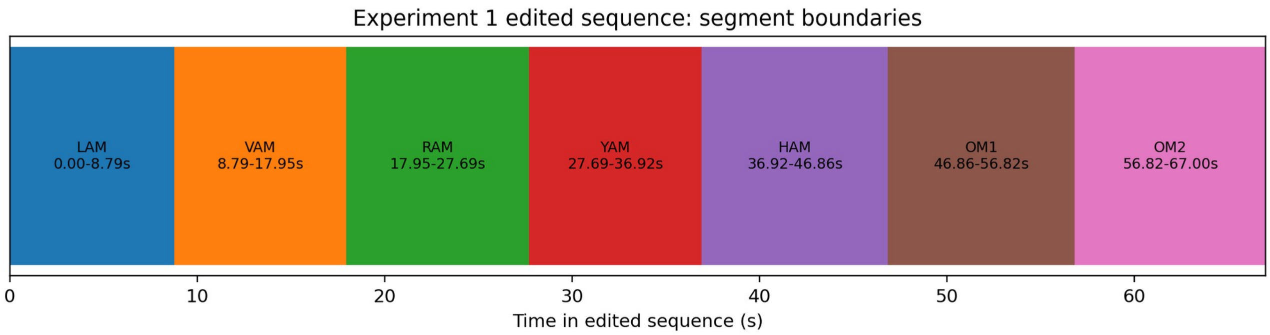

Figure 1. Segment timing in the 67 s edited Experiment 1 sequence.

3.3 Layered-OM Ājñā probe

Table 4. Separate layered-OM Ājñā probe metadata.

Parameter	Value
Video	om-ajna.mp4
Duration	9.920 s
Video stream	H.264, 1920 × 1080, 25 fps
Audio stream	AAC, stereo, 48 kHz
Stimulus construction	Original OM layered with a copy pitched down by one octave
Cymatic centre used for analysis	approximately x=947, y=307 px

3.4 Auxiliary RAM recording

Table 5. Auxiliary standalone RAM recording metadata.

Parameter	Value
Video	new-ram-chakras.mp4
Duration	10.080 s
Video stream	H.264, 1920 × 1080, 25 fps
Audio stream	AAC, stereo, 48 kHz
Purpose	Exploratory check for whether transient 10-fold organization appears in an additional RAM recording

4. Image-analysis method

The analysis was designed to reduce dependence on subjective 'petal counting'. A cymatic image can contain multiple simultaneous spatial scales: a large outer lobe pattern, an intermediate annular organization, and finer subdivisions. A global visual count may therefore miss a symmetry that is strong only at a particular radius.

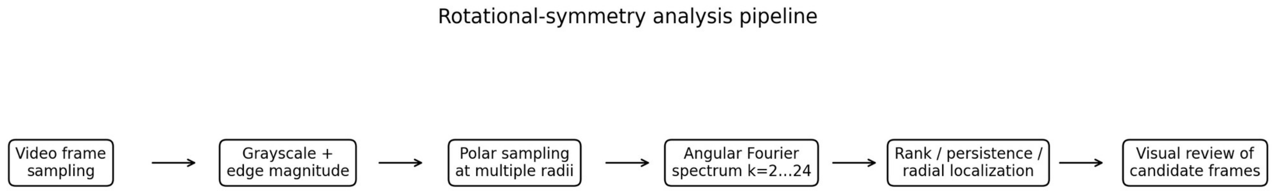

Figure 2. Analysis pipeline used to quantify rotational organization at multiple radial layers.

4.1 Pre-processing

- Frames were sampled throughout each bīja segment, with short boundary-adjacent intervals excluded where appropriate to reduce contamination by transitions between stimuli.
- Frames were converted to grayscale and lightly Gaussian-smoothed.
- Sobel x- and y-gradients were calculated and combined as gradient magnitude to emphasize geometric edges and radial structure rather than absolute illumination.
- A fixed cymatic centre was used for each video.

4.2 Polar radial sampling

For each frame, the gradient image was sampled around concentric circles centred on the cymatic field. Angular intensity traces were therefore obtained independently at multiple radii. This converts spatial organization around the centre into a one-dimensional periodic signal as a function of angle.

4.3 Angular Fourier decomposition

Each angular trace was mean-centred and normalized by its standard deviation before discrete Fourier transformation. Fourier magnitudes at rotational orders $k = 2$ through at least $k = 20$ (and, in earlier passes, through $k = 24$) were treated as symmetry-strength measures. A strong k component indicates repeated angular organization occurring approximately k times around that sampled radius. This general strategy is related to established rotational power-spectrum approaches used for objective analysis of rotationally symmetric images, although the present implementation is a custom exploratory pipeline.

4.4 Metrics

- Whole-section expected-order mean: mean strength of the traditional petal order across sampled frames and radii.
- Best-annulus mean: strength of the expected order in the strongest sustained radial band.
- Rank: position of the expected order relative to other rotational orders at the relevant frame/radius.
- Persistence: proportion of sampled frames in which an order ranked within the top three or first.
- Specificity/enrichment: comparison of a given order in its associated bīja section against the same order in the other first-five bīja sections.

- Nested correspondence: co-occurrence of different theoretically relevant rotational orders at different radial layers within the same frame or time window.

4.5 Why local radial analysis was necessary

The initial whole-section analysis correctly identified strong LAM/4 and HAM/16 relationships but understated RAM/10 and YAM/12. Subsequent radial decomposition showed that the traditional number need not be the visually dominant whole-field order. In RAM, 10-fold order can occur in a secondary radial layer while a 3/6 parent field dominates globally; in YAM, 6-fold and 12-fold organizations can coexist at different radii. The report therefore distinguishes global dominance from local structural correspondence.

5. Results: whole-section baseline

Table 6. First-pass whole-section expected-order metrics. These values describe the expected petal order before deeper radial-layer analysis.

Bīja	Expected order	Global mean expected-order score	Expected order in top 3 (%)	Median rank	Best-annulus mean	Relative enrichment vs other bījas
LAM	4	0.331	97.56	2.000	0.560	1.710
VAM	6	0.232	28.57	6.000	0.378	0.960
RAM	10	0.139	2.220	12.00	0.256	0.626
YAM	12	0.135	0.000	16.00	0.226	0.880
HAM	16	0.172	45.65	6.500	0.316	1.310

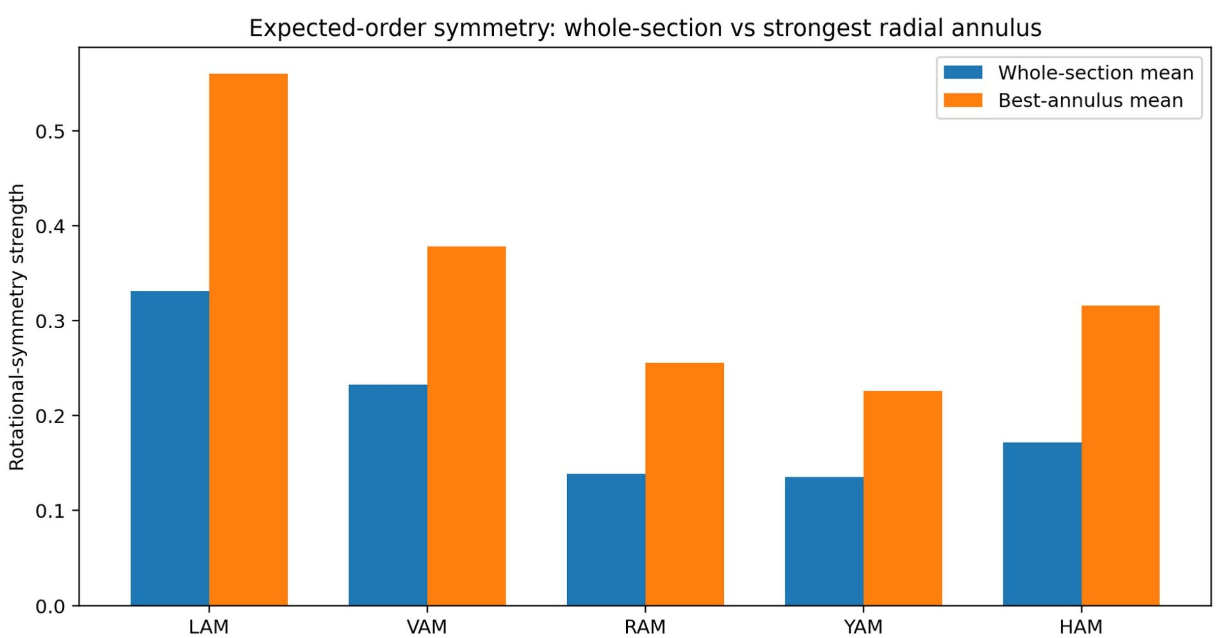

Figure 3. Expected rotational order measured as a whole-section average versus the strongest radial annulus.

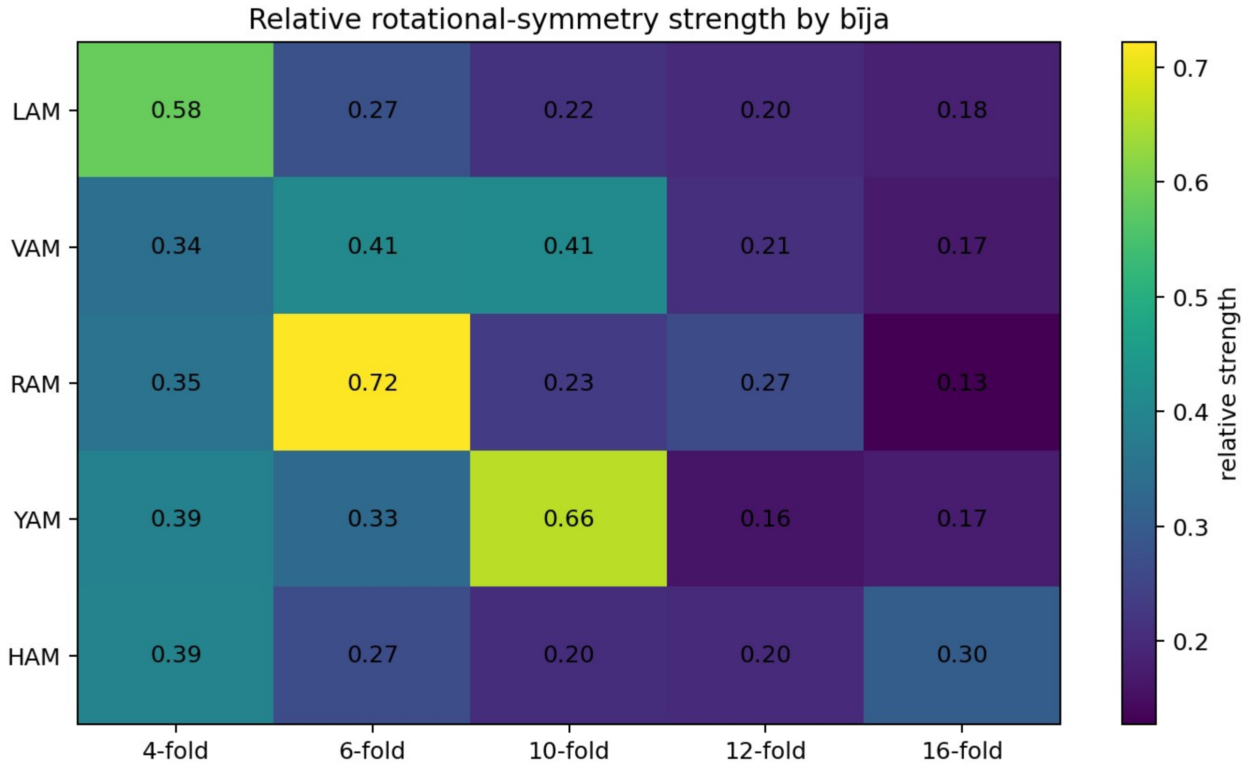

Figure 4. Cross-bīja relative rotational-symmetry matrix used in the specificity analysis. Rows are bīja sections; columns are candidate rotational orders. The matrix demonstrates both matches and displacement effects (notably strong 6-fold in RAM and strong 10-fold in YAM).

The baseline results produced an intentionally mixed pattern. LAM/4 was strong and highly persistent; HAM/16 was enriched relative to the same order in other bījas; VAM/6 appeared but was not selective; RAM/10 and YAM/12 were weak when treated as whole-section dominant orders. This mixed result is important because it argues against a trivial analysis in which every traditional number was visually or computationally forced to match.

6. Results by bīja and chakra comparator

6.1 LAM / Mūlādhāra: fourfold organization

The strongest and cleanest expected-order result in the primary sequence occurred during LAM. In the first-pass analysis, the 4-fold component had a whole-section mean score of approximately 0.331, ranked within the top three symmetries in approximately 97.6% of sampled frames, and had a median rank of 2. Its strongest sustained annulus had a mean score of approximately 0.560. The 4-fold signal was approximately 1.71 times the average 4-fold score observed across the other first-five bījas.

Multi-radius analysis localized the strongest fourfold field broadly to the middle region of the cymatic image, approximately 120–170 px from the centre in the later pass. Candidate frames repeatedly show four large sectors or chambers rather than only a fine 4-fold harmonic. This is therefore classified as a strong primary structural correspondence.

The traditional Mūlādhāra description also includes a square earth mandala. Some frames show orthogonal/four-cornered organization, but a literal square is not sufficiently stable or unambiguous to count as an independent quantitative match. The report therefore treats '4' as supported and 'square-like' as a secondary visual suggestion only.

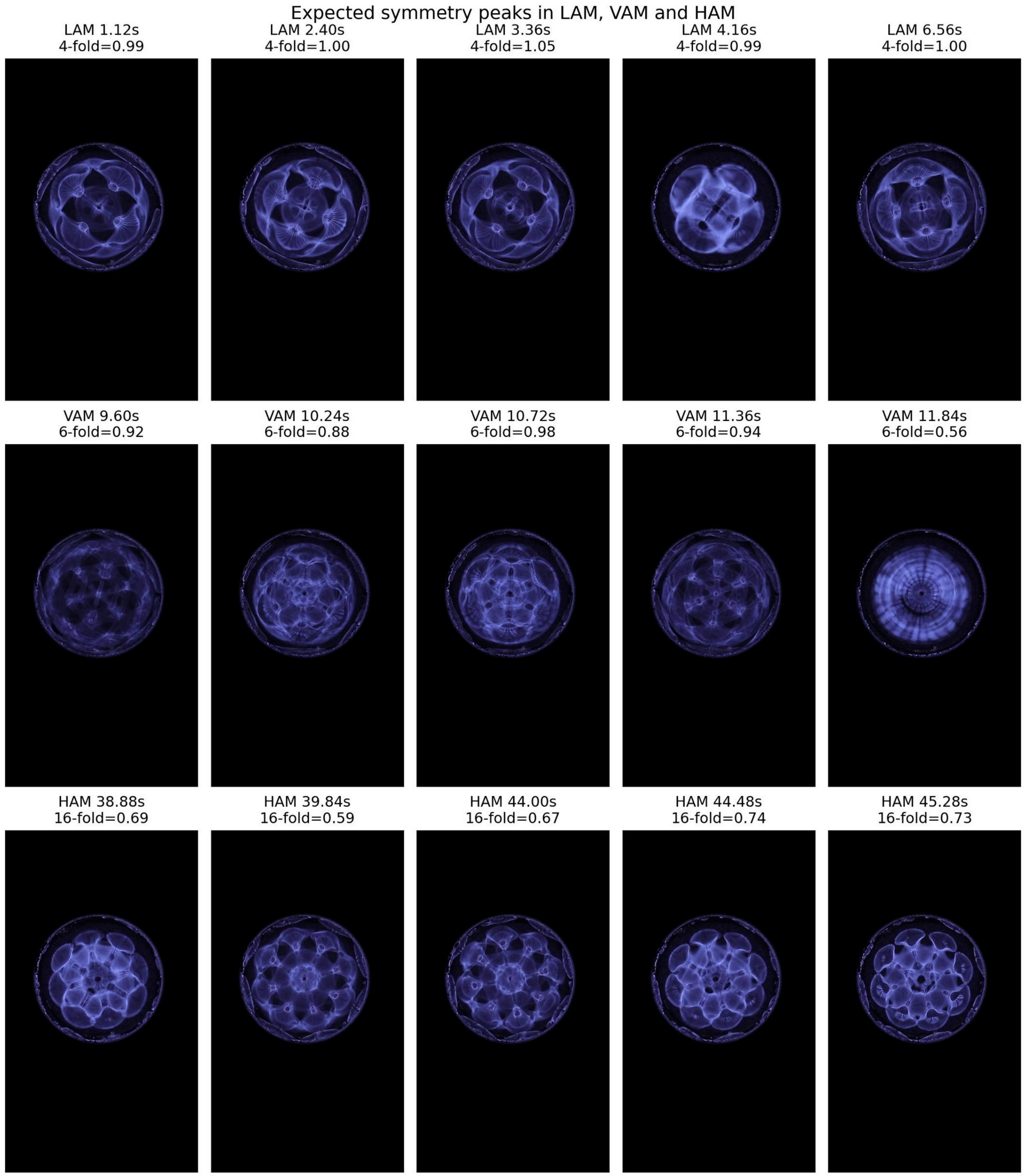

Figure 5. Strong expected-order candidate frames for LAM (top row), VAM (middle row), and HAM (bottom row). LAM repeatedly exhibits large-scale fourfold organization; VAM contains a pronounced sixfold phase; HAM shows high-order structured subdivision.

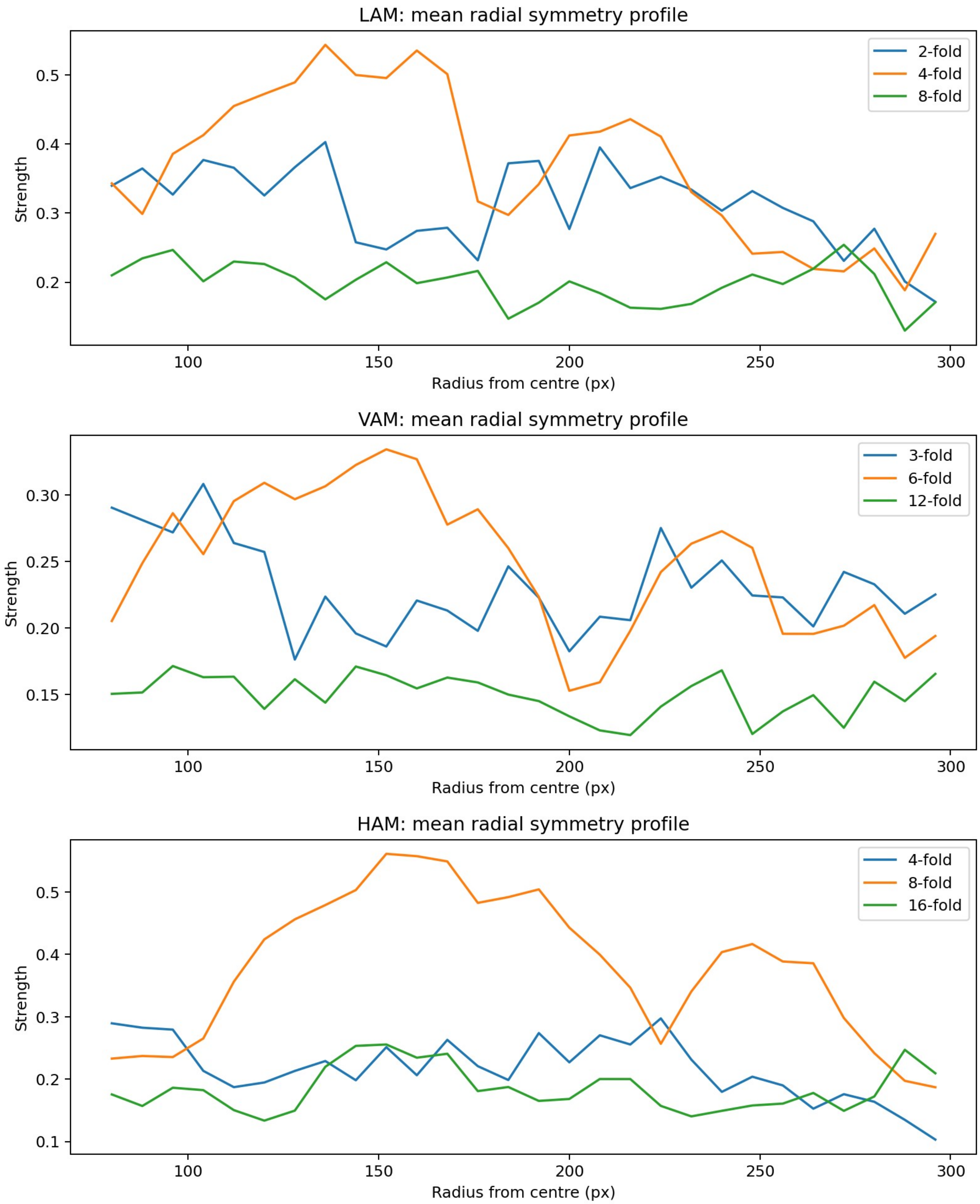

Figure 6. Mean radial symmetry profiles for LAM, VAM, and HAM. The LAM panel shows 4-fold dominance across a broad middle radial band; the VAM panel shows a distinct 6-fold band; the HAM panel shows a strong 8-fold parent architecture with 16-fold higher-order structure.

6.2 VAM / Svādhiṣṭhāna: transient sixfold organization

VAM produced a clear and visually coherent sixfold phase, concentrated particularly around approximately 9.6-11.4 s of the edited sequence. In the first-pass whole-section analysis, the expected 6-fold component had a mean score of approximately 0.232 and a best-annulus mean of approximately

0.378. It entered the top three rotational orders in approximately 28.6% of sampled frames, with a median rank of 6. The whole-section statistics therefore understate the strongest VAM interval: targeted temporal and radial inspection shows a sustained period in which six large-scale sectors or chambers organize the middle field rather than appearing only as a weak high-order harmonic.

The refined radial profile localizes this correspondence to a broad middle annulus, approximately 120-175 px from the cymatic centre, where 6-fold organization consistently exceeds the neighbouring 3-fold and 12-fold components. Strong candidate frames occur at approximately 9.60, 10.24, 10.72, 11.36, and 11.84 s, with local 6-fold strengths reaching approximately 0.88-0.98 in the later analysis. Visually, these frames show six broad lobes or chambers around the centre, supporting interpretation of the 6-fold component as a primary transient architecture rather than merely a numerical Fourier artifact.

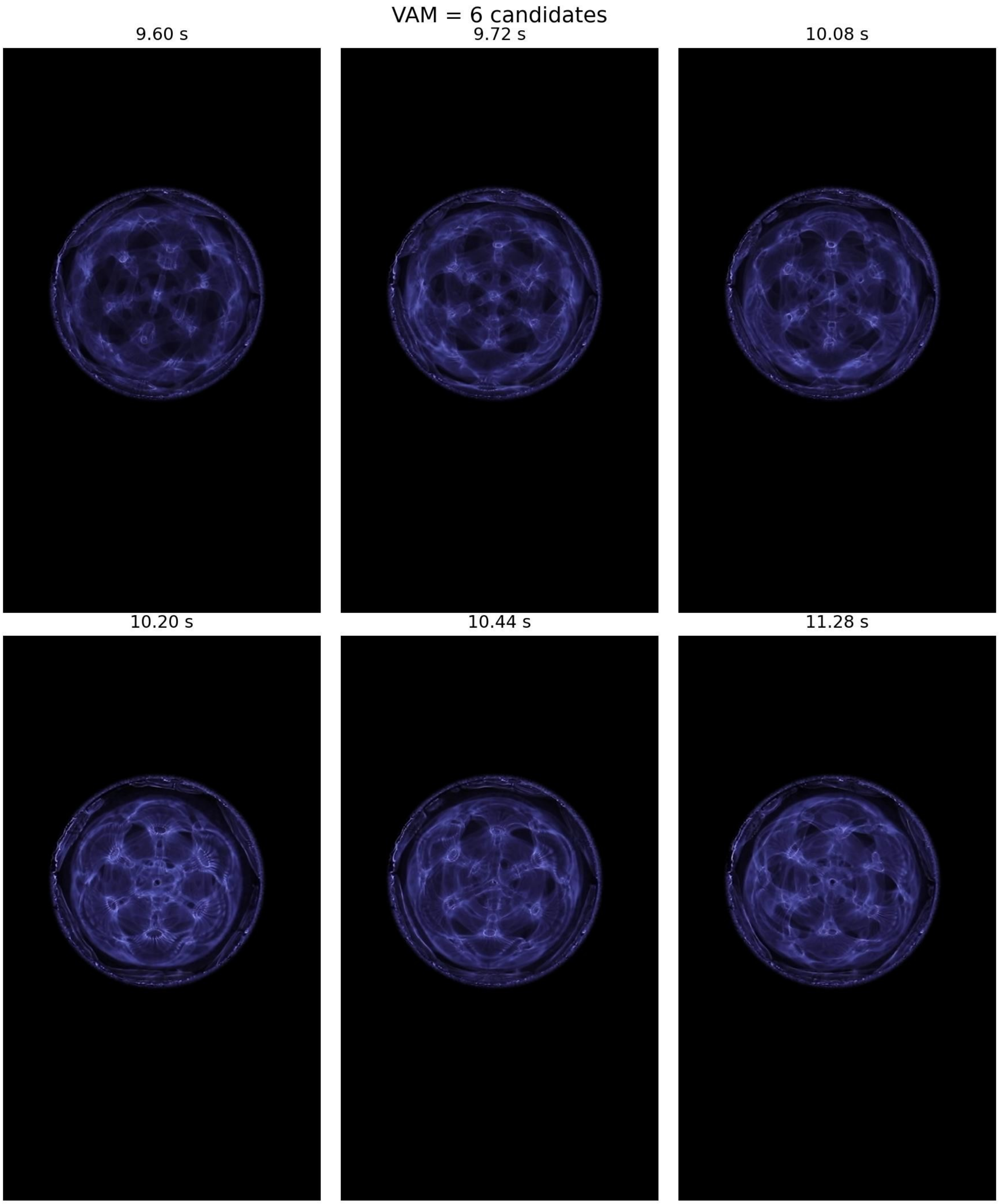

Figure 7A. Dedicated VAM/Svādhiṣṭhāna sixfold candidate sequence. The strongest interval shows repeated six-part organization of the middle cymatic field, especially during approximately 9.6-11.4 s.

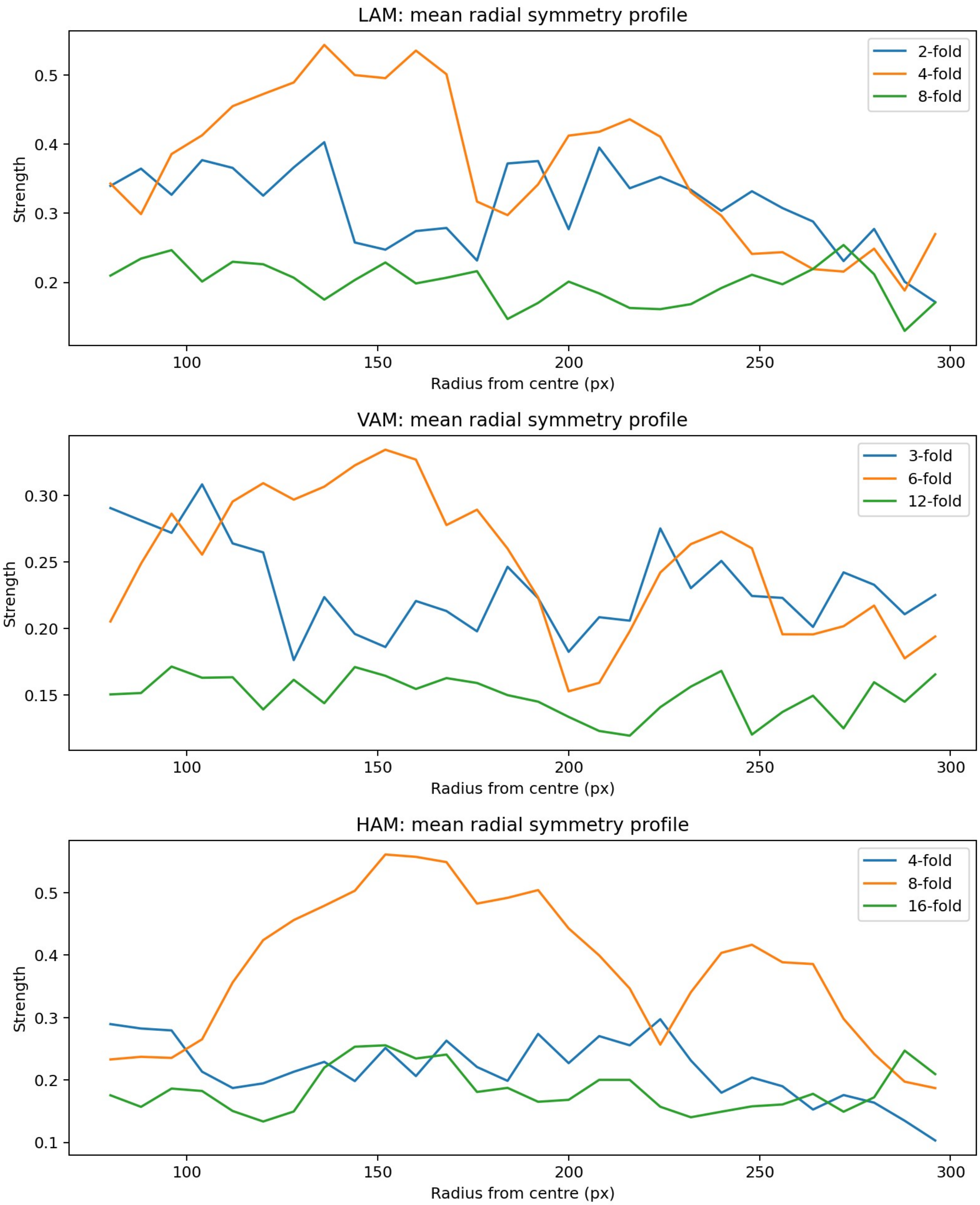

Figure 7B. Radial symmetry profiles including VAM. In the VAM panel, 6-fold order forms a broad dominant middle-radius band, approximately 120-175 px, relative to the 3- and 12-fold comparison orders.

6.3 RAM / Maṇipūra: 3→6 parent field with a separate 10-fold layer

RAM initially appeared to be a mismatch. Its expected 10-fold order had a low whole-section mean of approximately 0.139, was in the top three symmetries in only approximately 2.2% of sampled frames, and had a median rank of 12. By contrast, 6-fold organization was the dominant whole-section order.

Targeted multi-radius analysis changed the interpretation. Repeated candidate intervals showed strong local 3-fold organization together with very strong 6-fold organization. Examples included approximately 18.52 s (3-fold ≈ 0.81), 19.96 s (3-fold ≈ 0.84 with 6-fold ≈ 0.99), 21.24 s (3-fold ≈ 0.87 with 6-fold ≈ 0.97), and 23.88 s (3-fold ≈ 0.82 with 6-fold ≈ 0.99). This supports a 3/6 parent relationship rather than treating sixfold structure as simply 'incorrect' for RAM.

At separate radii in the same RAM field, 10-fold organization rose transiently to approximately 0.5–0.66. The first RAM sequence also contained a particularly clear 10-fold episode around approximately 21.36–21.92 s, where 10-fold became locally dominant at a middle radial band near ~330 px in the earlier analysis. Thus RAM is best described as a dominant 3→6 parent field with a real but secondary 10-fold radial organization.

This creates a structural parallel with the traditional Maṇipūra combination of a triangular fire mandala and ten-petalled lotus, while remaining short of a literal claim that the water reproduces the historical diagram.

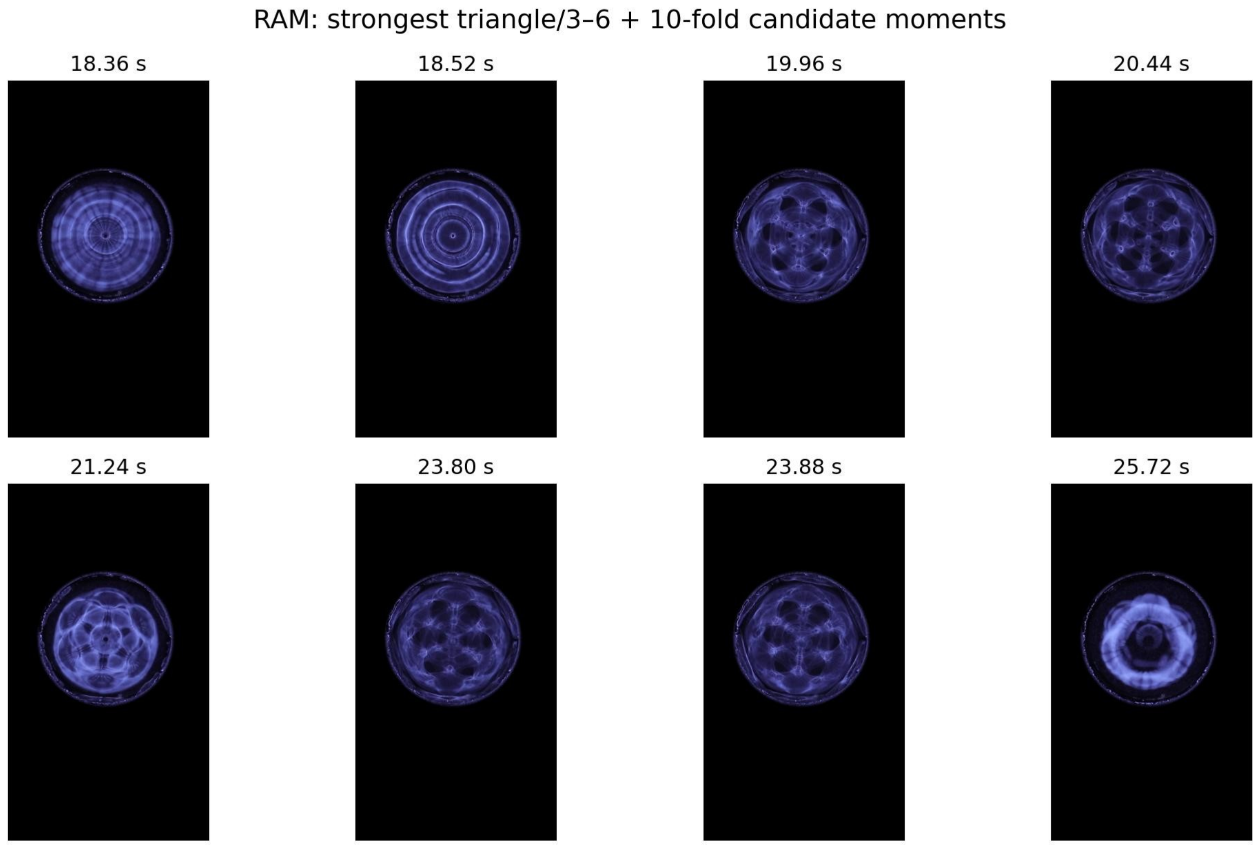

Figure 7. RAM candidate frames selected for simultaneous triangle-related 3/6 structure and local 10-fold organization.

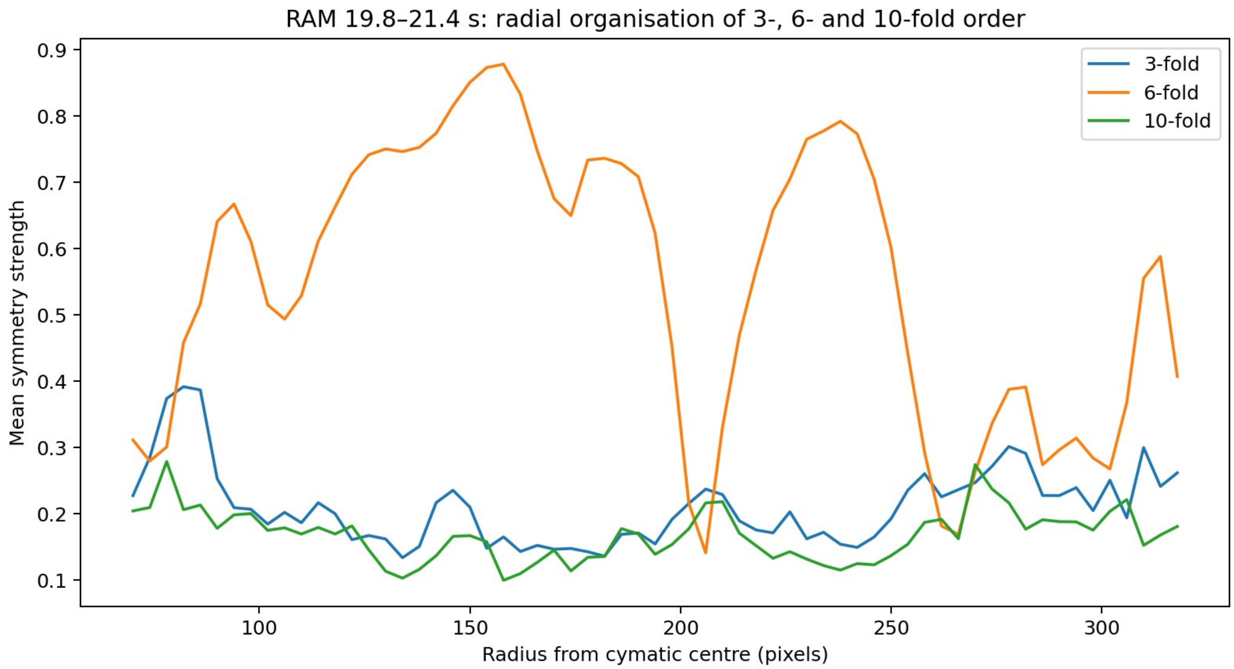

Figure 8. RAM radial profile during 19.8–21.4 s. Sixfold organization dominates broad radial regions while 3-fold and 10-fold components remain localized at other radii.

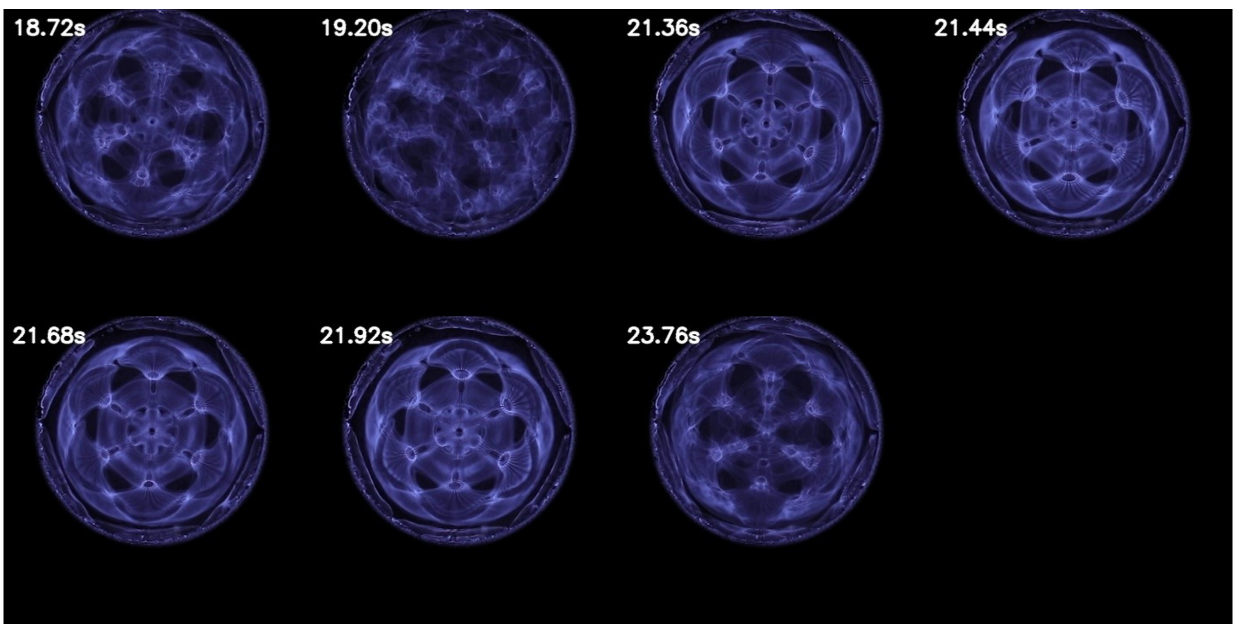

Figure 9. Targeted 10-fold candidate frames from the first RAM recording. The 10-fold component is not the obvious outer lobe count; it is localized to a secondary radial architecture.

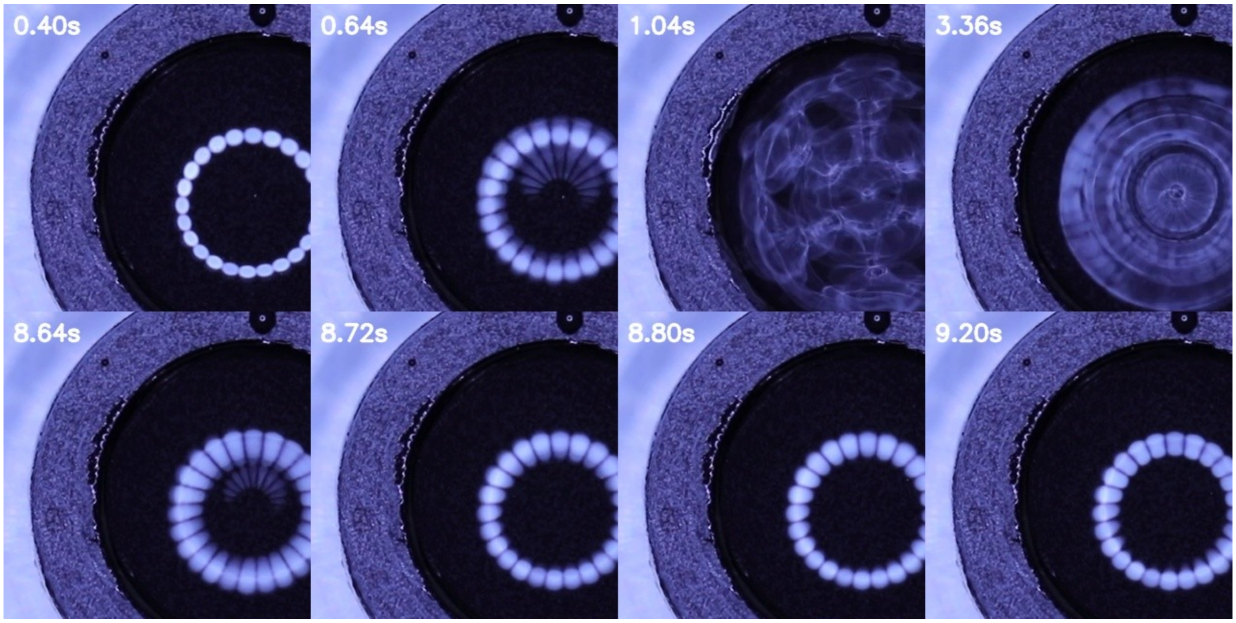

Figure 10. Auxiliary standalone RAM recording: strongest 10-fold candidate frames. Tenfold order is again detectable transiently but remains secondary to lower-order structure.

6.4 YAM / Anāhata: nested 6-fold and 12-fold organization

The initial whole-section analysis also made YAM appear discordant: expected 12-fold order had a mean score of approximately 0.135, never ranked within the top three in that first global pass, and had a median rank of 16, while 10-fold organization dominated the section.

Radial-layer analysis identified a more specific relationship. During approximately 34.4–35.1 s, strong 6-fold organization occurred closer to the centre while 12-fold order strengthened at a more external radius within the same frames. At approximately 34.42 s, 6-fold peaked near 98 px and 12-fold near 202 px. At approximately 34.98–35.06 s, 6-fold peaked near 122–126 px while 12-fold peaked near 250 px. At approximately 34.74 s, the local 12-fold component was the strongest symmetry at its sampled radius; at other candidate moments it ranked second or third.

This nested organization is especially relevant because the traditional Anāhata model combines a twelve-petalled lotus with a six-cornered inner mandala. The result is therefore classified as a strong layered structural parallel rather than a globally dominant 12-fold field.

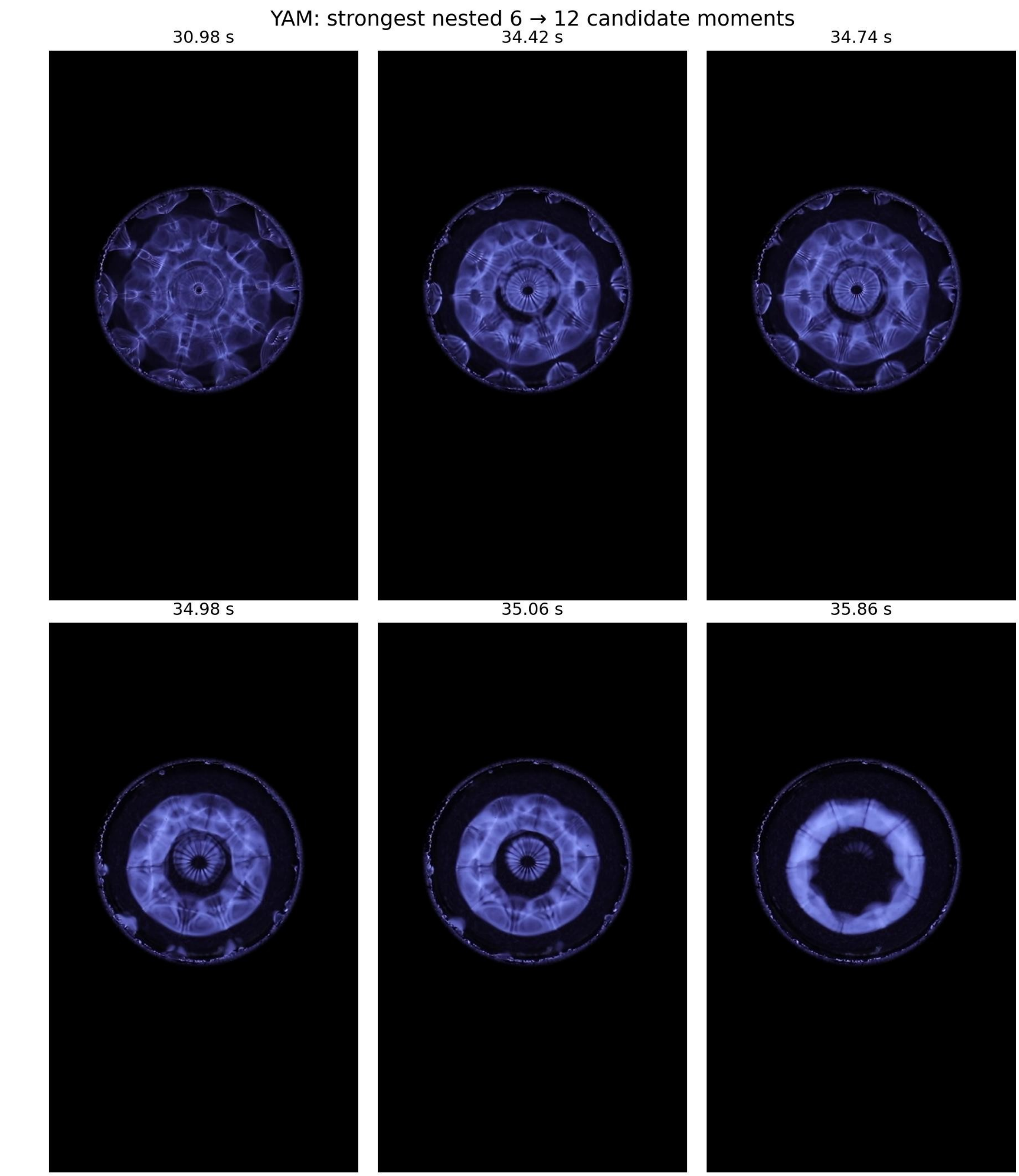

Figure 11. YAM candidate frames with simultaneous or near-simultaneous 6-fold and 12-fold organization at different radial layers.

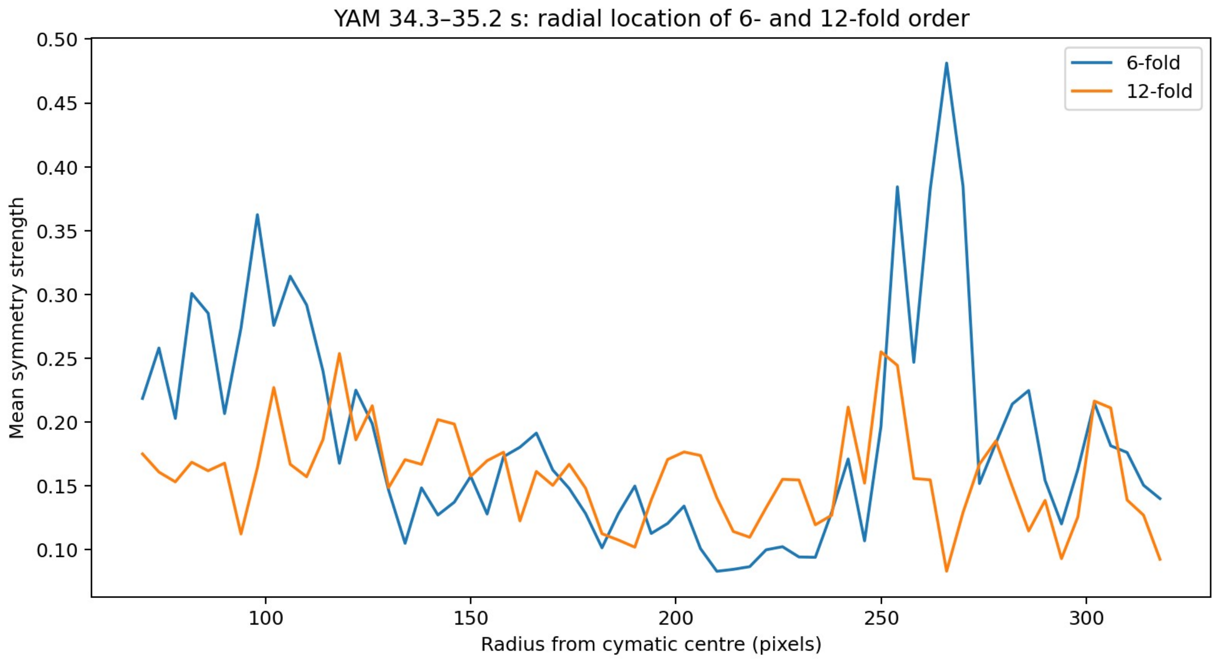

Figure 12. YAM radial profile for 34.3–35.2 s. Sixfold order dominates selected inner/middle regions while 12-fold order rises at distinct outer or intermediate radii.

6.5 HAM / Viśuddha: 8-fold parent structure with 16-fold subdivision

HAM showed one of the strongest expected higher-order relationships in the primary sequence. In the first-pass analysis, the 16-fold whole-section mean was approximately 0.172, the best-annulus mean was approximately 0.316, and 16-fold order entered the top three symmetries in approximately 45.7% of sampled frames. Relative to the same rotational order across the other first-five bīja sections, HAM/16 was enriched, making it one of the more selective expected-order findings in the experiment rather than merely a high-order component that occurs uniformly throughout the dataset.

The deeper radial analysis reveals a hierarchical structure rather than sixteen equally prominent outer petals. Eightfold organization is the dominant parent architecture across a broad middle radial region, approximately 110-210 px and particularly around 150-165 px. Sixteenfold order recurs as a finer subdivision superimposed on or emerging from that 8-fold parent form, with strong candidate intervals around approximately 38.9-39.8 s and again around 44.0-45.3 s. In the later local analysis, selected 16-fold strengths reached approximately 0.59-0.74. This 8→16 relationship is therefore interpreted as a primary lower-order scaffold carrying a meaningful higher-order subdivision.

The traditional Viśuddha model combines sixteen petals with a round ākāśa mandala. The measured 16-fold subdivision provides the useful numerical comparison. The circular/annular appearance itself is not counted as independent evidence because the experimental vessel is circular and therefore physically privileges annular and rotational modes. Treating the circle as a boundary-condition confound while retaining the selective 16-fold result is important to the conservative interpretation of this section.

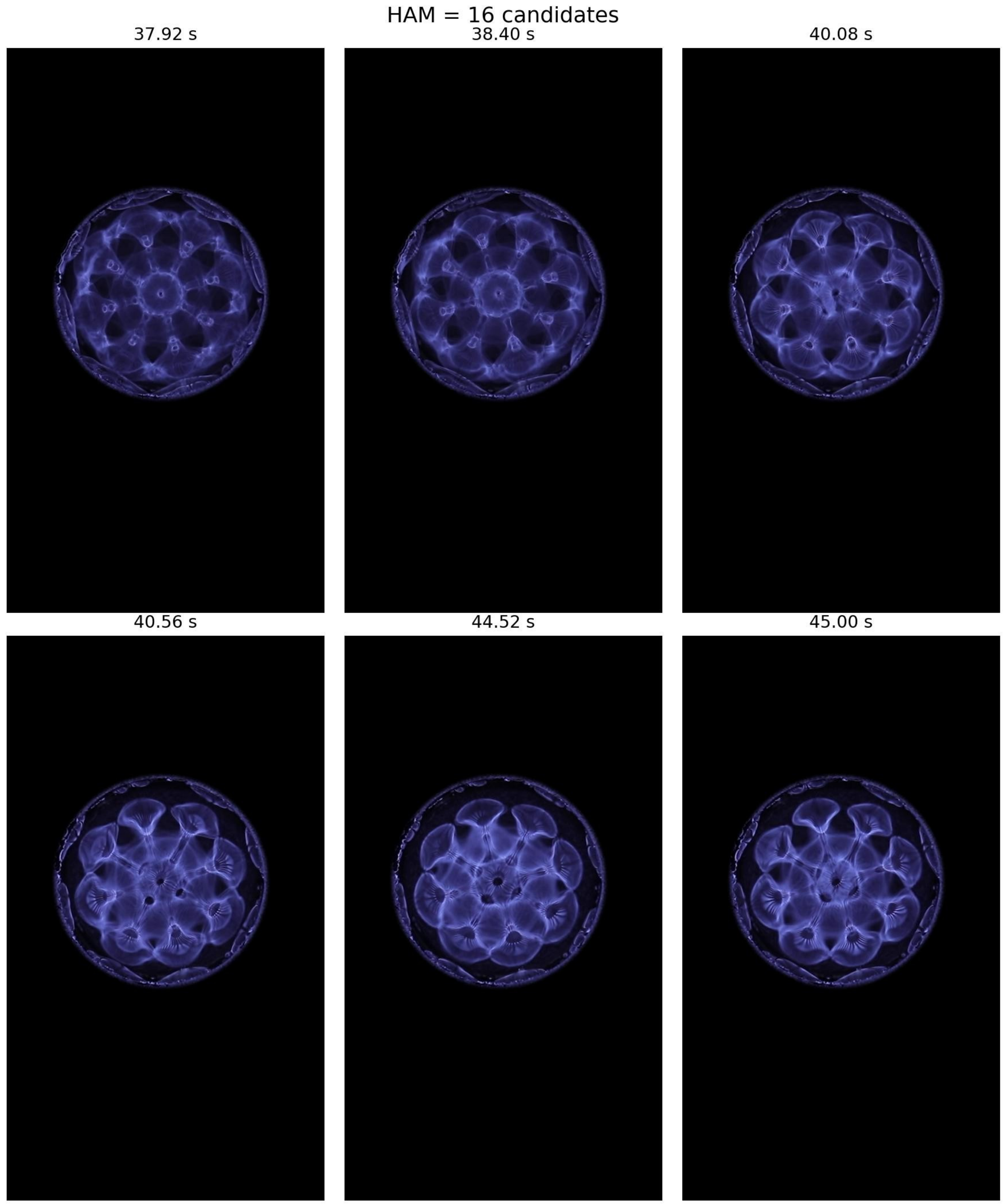

Figure 13A. Dedicated HAM/Viśuddha candidate sequence. Recurrent high-order subdivision is visible across the HAM interval, with particularly strong 16-fold episodes in the later portion of the segment.

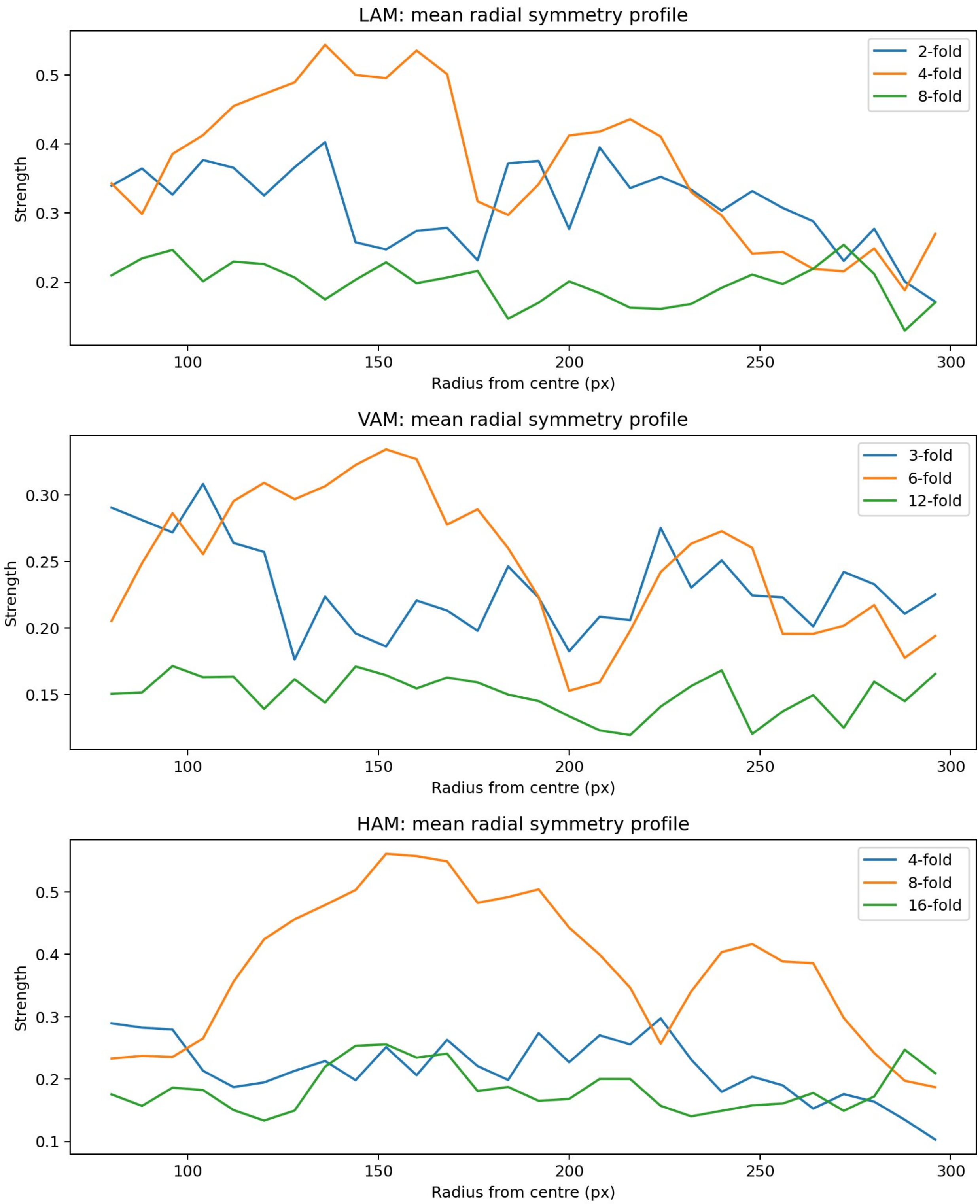

Figure 13B. Radial symmetry profiles including HAM. The HAM panel shows a strong 8-fold parent field across the middle radii with a recurring 16-fold higher-order component, supporting an 8→16 hierarchical interpretation.

6.6 OM and Ājñā: effect of octave layering on twofold organization

The original OM sections of the 67 s sequence showed nested higher-order organization, including strong 8-, 16-, and 24-fold components, and the two repeated OM excerpts displayed highly similar visual architecture. In earlier analysis, corresponding frames across the repeated OM sections showed high image similarity, consistent with the experimenter's observation that repeated identical inputs tend to retrace the same pattern family. However, the original OM did not display a strong persistent twofold organization.

The separate Ājñā probe deliberately changed the stimulus by layering the original OM with a copy pitched down by one octave. In this layered recording, 2-fold organization became the strongest overall low-order symmetry. Across the active section, 2-fold was the top-ranked symmetry in approximately 46% of sampled frames, occurred within the top three in approximately 90%, and had a median rank of approximately 2. By comparison, the earlier single-OM analysis showed substantially weaker and less persistent twofold organization.

Radially, the innermost region of the layered OM was especially dominated by 2-fold order. Moving outward, the field became mixed 2/4, and more external regions showed stronger 4-fold with secondary 8-fold structure. Sixteenfold order remained comparatively weak. The result therefore supports a central twofold architecture rather than a literal whole-bowl two-petal drawing.

The conceptual parallel is notable: one OM is presented simultaneously at two octave-related pitch levels, and the resulting central field becomes strongly bilateral/twofold. This is retained as an interpretive observation only. The experiment does not establish that octave pairing causes a two-petalled geometry or that the traditional Ājñā image encodes an octave relation.

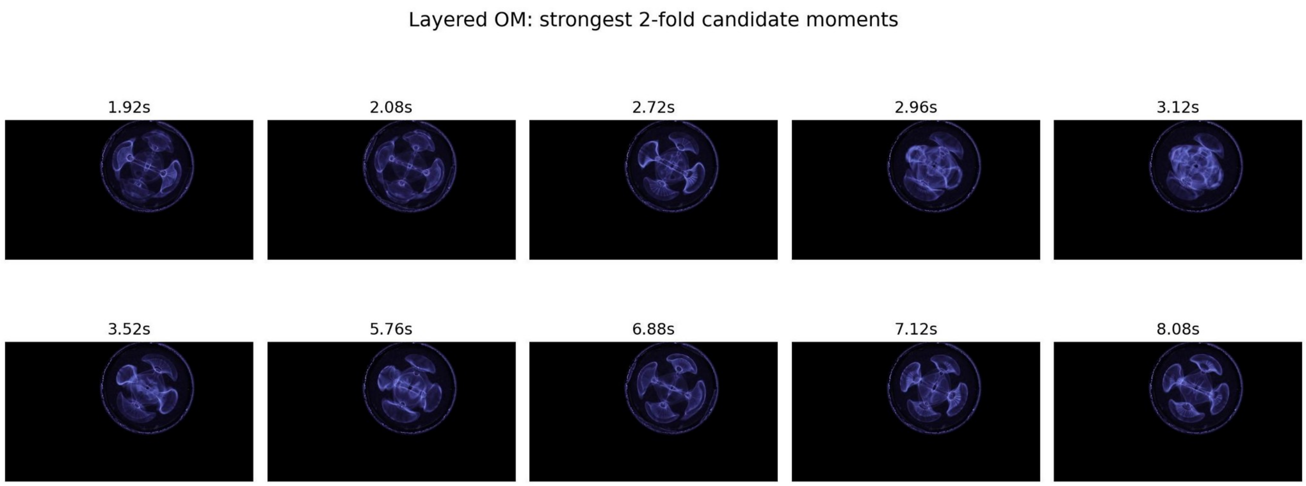

Figure 13. Layered OM: strongest candidate moments for persistent twofold/bilateral organization relevant to the Ājñā comparison.

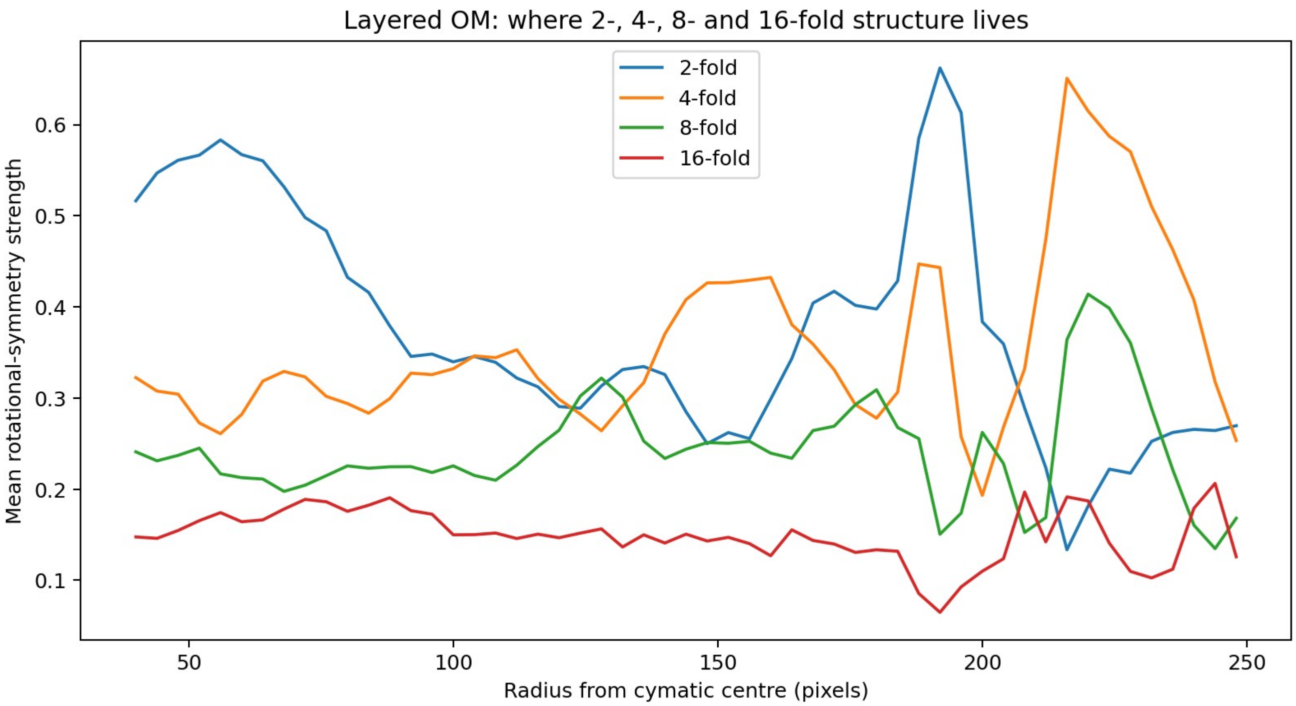

Figure 14. Layered OM radial hierarchy. Twofold order is strongest in the inner field; 4-fold and 8-fold organization become more important at larger radii.

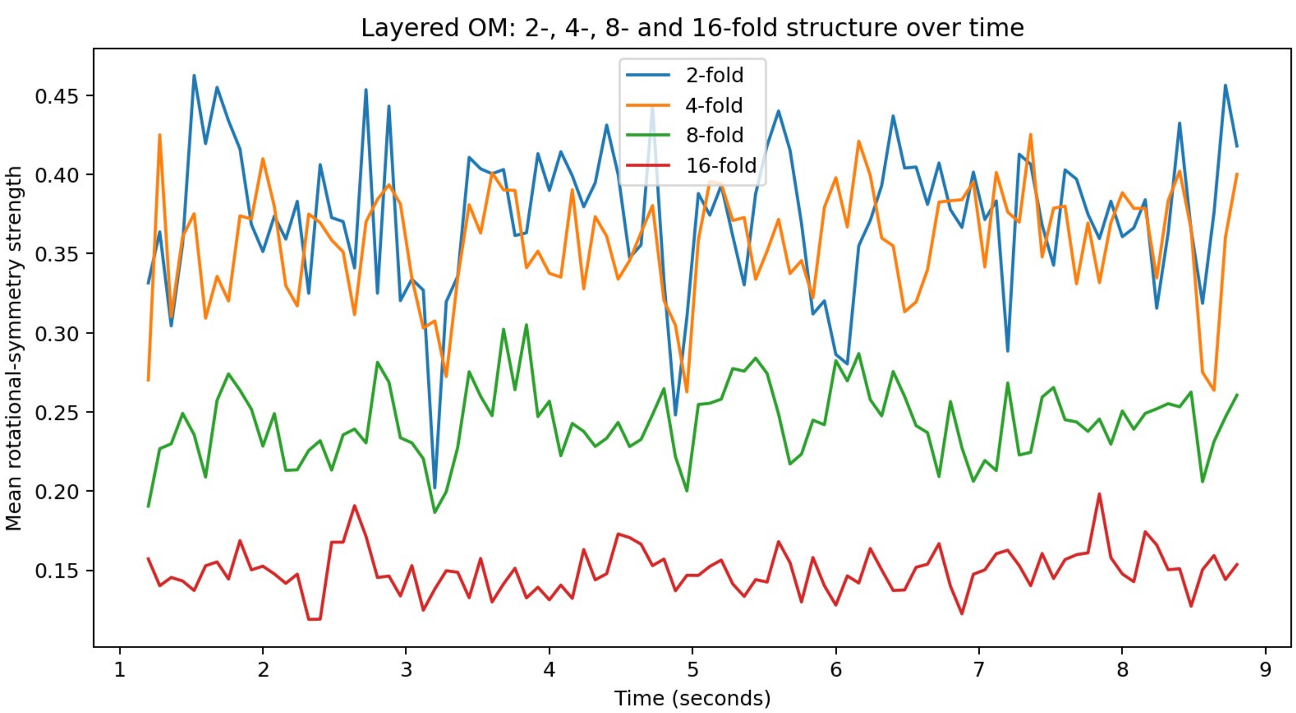

Figure 15. Layered OM temporal profile. Twofold and fourfold orders remain dominant across much of the active recording rather than appearing as a single isolated frame.

6.7 OM / Sahasrāra: radial multiplicity, subdivision, and repeatable high-order organization

The final OM observation was analysed as a Sahasrāra probe. Unlike the lower centres, the traditional Sahasrāra is represented as a thousand-petalled lotus. The present experiment does not treat 1,000 as a literal rotational-symmetry target. Instead, the physical comparison is whether unmodified OM produces a field distinguished by unusually dense radial multiplicity, nested subdivision, coexistence of multiple rotational orders, and repeatable high-order architecture.

The resulting field is not dominated by one simple petal count. Its spectrum is organized around a persistent 4/8/16/24 family, with 8-fold structure strongest overall and 16- and 24-fold components retained as higher-order subdivisions. Across the observation, approximately eleven rotational orders exceeded the working material-expression threshold on average. Radial analysis showed that these orders occupy different spatial bands rather than collapsing into one global symmetry: lower-order organization is stronger closer to the centre, while 8-, 16-, and 24-fold structure becomes prominent across intermediate and outer radial zones.

The Sahasrāra observation also showed exceptionally strong empirical repeatability when the same OM stimulus was repeated under unchanged apparatus conditions. Repeated presentations produced a mean rotational-spectrum correlation of approximately 0.997, closely matched global complexity measures, strong matched-frame similarity, and correlated temporal trajectories of spectral complexity. These repetitions are treated here as an internal repeatability check for one OM/Sahasrāra observation, not as separate chakra conditions.

Accordingly, the Sahasrāra result is classified as a strong conceptual/structural correspondence through radial multiplicity and subdivision, with exceptionally strong empirical repeatability. The correspondence is not that OM literally produces one thousand visible petals; rather, the cymatic field shifts toward a densely differentiated, multi-order radial architecture that is qualitatively and quantitatively distinct from the simpler low-order organizations observed elsewhere in the sequence.

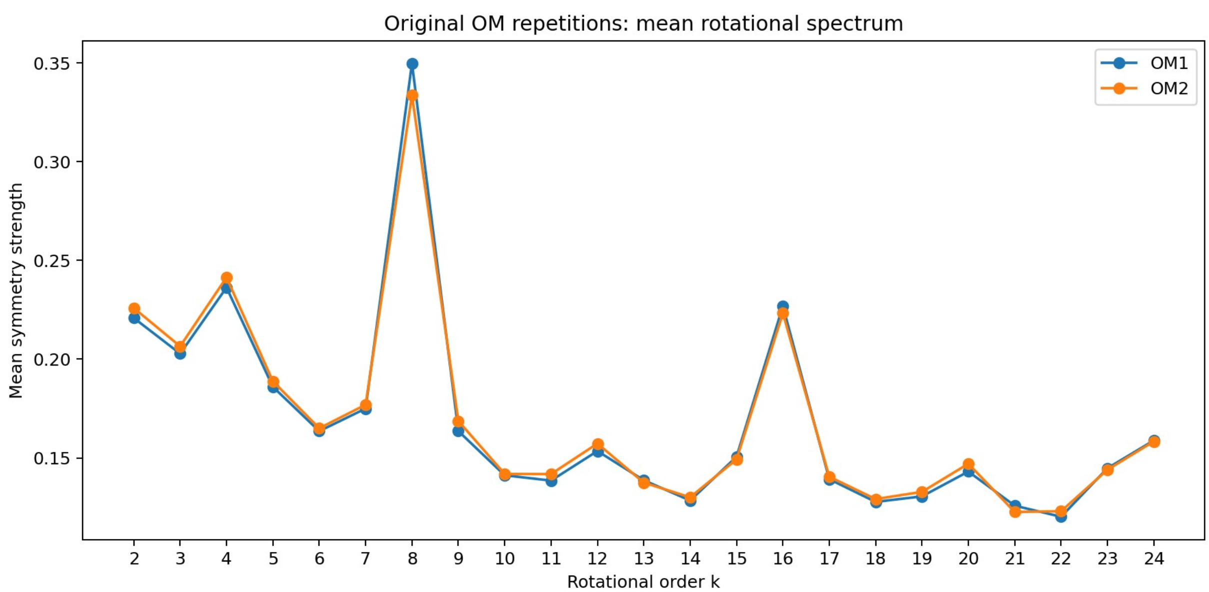

Figure 16. Unmodified OM/Sahasrāra rotational spectrum. The observation is characterized by a persistent multi-order hierarchy dominated by 8-fold structure with substantial 4-, 16-, and 24-fold components.

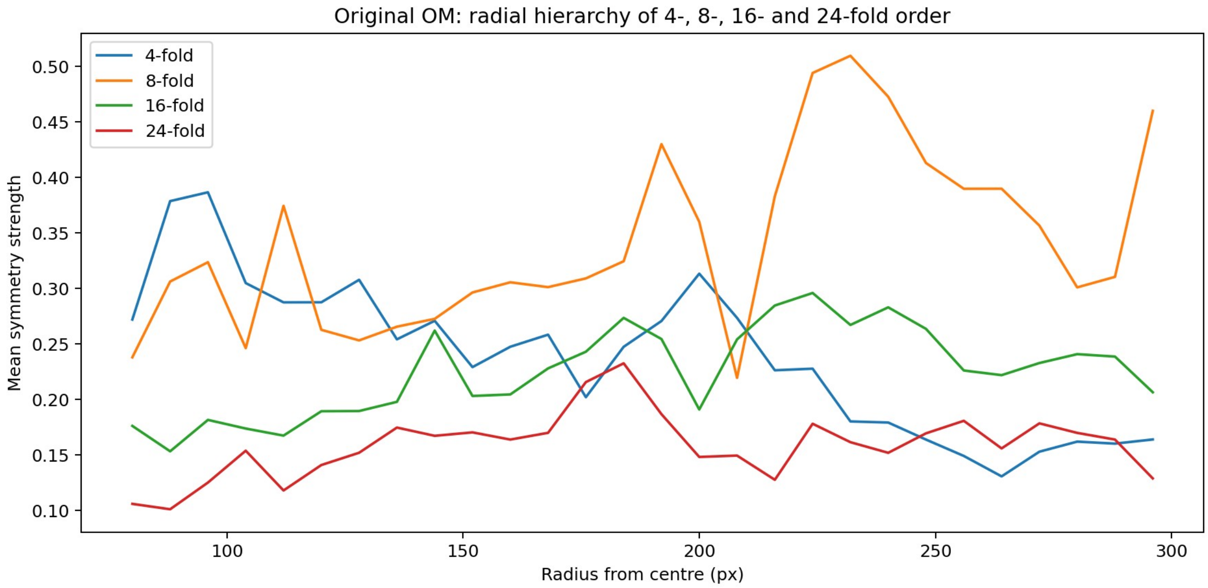

Figure 17. OM/Sahasrāra radial hierarchy. Different rotational orders occupy different radial bands, demonstrating spatial subdivision rather than a single global symmetry.

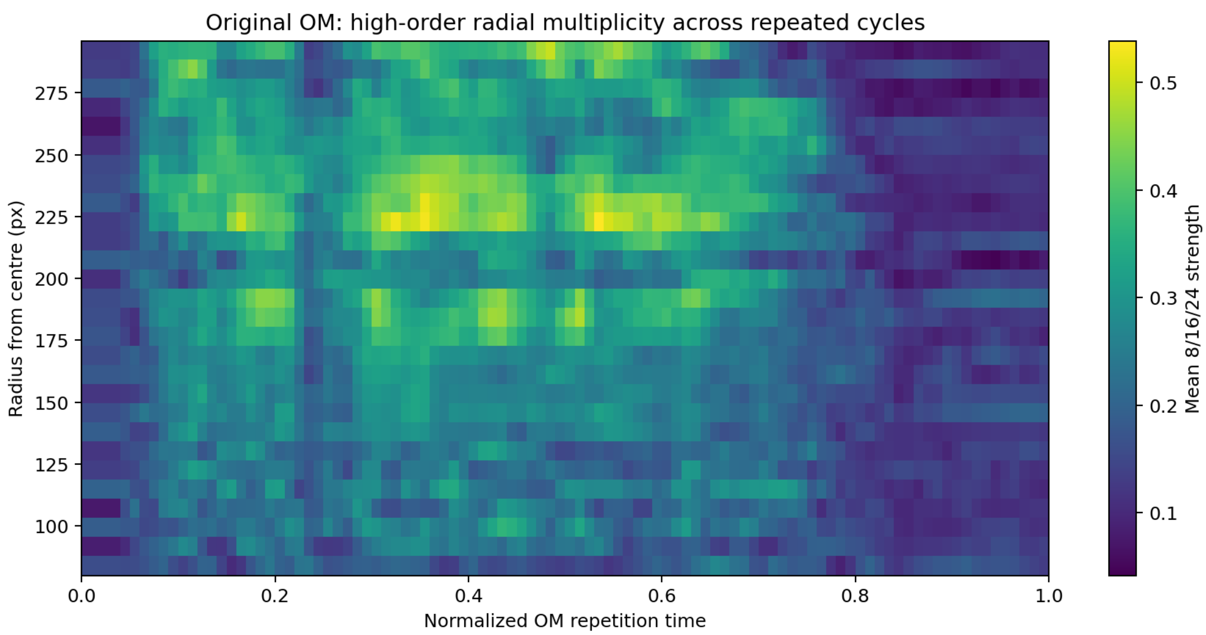

Figure 18. High-order OM/Sahasrāra radial multiplicity. The heat map shows simultaneous and spatially distributed 8-, 16-, and 24-fold organization.

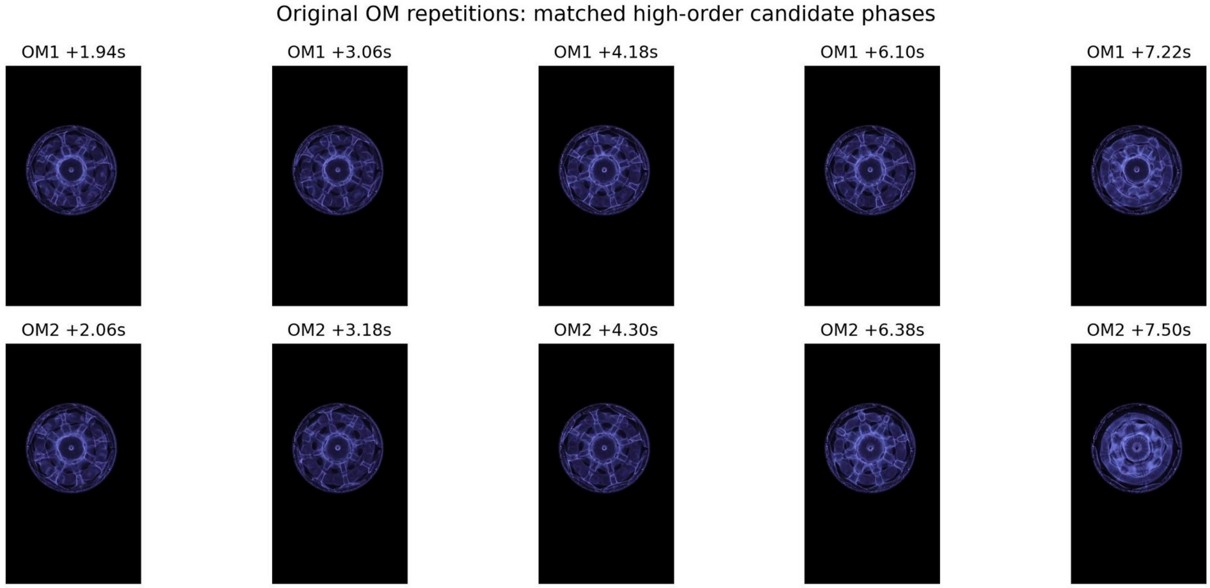

Figure 19. Representative matched phases from repeated presentations of the same unmodified OM stimulus. The repetitions serve as an internal repeatability check for the single Sahasrāra observation.

7. Integrated structural interpretation

Table 7. Integrated evidence map after multi-radius analysis.

Centre	Stimulus	Traditional number	Observed architecture	Current assessment	Important caveat
Mūlādhāra	LAM	4	Strong primary 4-fold field	Very strong	Square-like organization suggestive only
Svādhiṣṭhāna	VAM	6	Clear transient 6-fold band	Strong	Not selective; curvature qualitative
Maṇipūra	RAM	10	3→6 parent + separate 10-fold layer	Moderate-strong layered	Global 10 weak
Anāhata	YAM	12	Inner/mid 6 + outer/local 12	Strong layered	Global 12 weak; 10 dominates whole section
Viśuddha	HAM	16	8 parent → 16 subdivision	Very strong	Circle confounded by bowl
Ājñā	OM + octave	2	Persistent central 2-fold field	Very strong	Stimulus differs from original OM
Sahasrāra	OM	1000 / innumerable	Dense multi-order 4/8/16/24 radial field	Strong conceptual/structural	Multiplicity, not literal k=1000

Current structural correspondence map

Centre	Stimulus	Petal-order correspondence	Yantra/parent correspondence
Mūlādhāra	LAM	Strong primary	4-fold; square suggestive
Svādhiṣṭhāna	VAM	Strong transient primary	Curved/annular; crescent suggestive
Maṇipūra	RAM	Secondary/local	3→6 parent; triangle-related
Anāhata	YAM	Nested/local	6-fold inner + 12 outer
Viśuddha	HAM	Strong higher-order	8→16; circle confounded
Ājñā	OM + octave	Strong central	2-fold central; 4/8 outward

Figure 16. Condensed structural correspondence map after completion of the multi-radius analysis.

7.1 The central finding: relevant orders occur at different spatial scales

The most important analytical development was the realization that the traditional numerical or geometric correspondence, when present, does not occupy the same spatial scale for every centre. LAM expresses 4-fold order as an obvious large-scale field. VAM shows a transient primary 6-fold band. RAM expresses 10-fold order as a secondary layer inside a dominant 3/6 architecture. YAM expresses 6 and 12 at different radii. HAM expresses 16 as higher-order subdivision of an 8-fold parent form. In layered OM/Ājñā, 2-fold order is strongest centrally while 4 and 8 become more prominent outward. In unmodified OM/Sahasrāra, the field no longer reduces meaningfully to one low-order count and instead displays dense multi-order radial subdivision, especially a persistent 4/8/16/24 hierarchy.

This suggests that a useful hypothesis for subsequent work is not 'each bīja draws the same number of visible outer petals as its chakra diagram' but rather that bīja-driven cymatic fields may organize characteristic rotational orders at specific spatial scales, while the Sahasrāra/OM condition may be distinguished by the degree of radial multiplicity and subdivision itself.

7.2 Positive results are strengthened by non-matches

The dataset contains several findings that do not conform neatly to the traditional petal sequence. RAM is globally dominated by 6-fold rather than 10-fold order; YAM is globally dominated by 10-fold rather than 12-fold order; VAM/6 is not selective because 6-fold is strong in RAM; and a traditional circular motif cannot be meaningfully claimed for Viśuddha because the bowl is circular. These deviations are scientifically valuable. They reduce the likelihood that the result is merely the consequence of selecting one attractive frame per mantra and labeling it according to expectation.

8. Discussion

8.1 What the experiment supports

- The six bīja sections do not produce one uniform symmetry family; their dominant and local rotational organizations differ within a fixed apparatus.
- Some traditional numerical orders are strongly expressed: LAM/4, HAM/16, and layered-OM/2 are the clearest.

- Other comparisons become meaningful only after spatial decomposition: RAM/10 and YAM/12 are examples.
- Traditional parent geometry can coincide with a different dominant rotational order: RAM shows strong 3/6 structure; YAM shows a 6/12 layered relationship.
- Rotational symmetry in the water is hierarchical: lower-order parent forms and higher-order subdivisions can coexist in the same frame.
- The unmodified OM/Sahasrāra observation combines dense multi-order radial subdivision with exceptionally strong empirical repeatability, making reproducibility itself one of the principal findings of Experiment 1.

8.2 What the experiment does not support

- It does not prove the physical existence of chakras as anatomical or measurable biological structures.
- It does not establish that historical chakra diagrams were derived from cymatic experiments.
- It does not show that each bīja uniquely produces only its traditional petal number.
- It does not establish a causal relationship between mantra meaning and water geometry.
- It does not yet distinguish the effects of phoneme, pitch, spectral envelope, amplitude modulation, duration, or harmonic content.
- It does not yet demonstrate generalization across different bowls, water depths, transducers, playback levels, voices, or laboratories.

8.3 Physical interpretation

From a physical perspective, the cymatic field is expected to emerge from coupled forcing, fluid motion, resonance, boundary conditions, and nonlinear interaction between modes. A circular vessel can privilege annular and rotational structures, and harmonic relationships between angular orders can produce apparent parent/subdivision relationships. These mechanisms do not negate the observed correspondences; they define the physical substrate that future experiments must characterize.

The present analysis is therefore most valuable where it identifies structured, testable relationships: for example, whether LAM repeatedly produces stronger 4-fold order than control syllables under identical forcing; whether YAM repeatedly shows a 6-inside-12 radial relationship; or whether HAM's 16-fold enrichment survives changes in pitch and apparatus.

8.4 Historical interpretation

The traditional chakra material combines phonetic, numerical, geometric, elemental, and contemplative symbolism. The present study compares only those aspects that can plausibly be operationalized in a cymatic image: rotational order, spatial hierarchy, and selected geometric relationships. Elemental and metaphysical meanings are not treated as measurable physical variables in this experiment.

9. Limitations and potential confounds

Table 8. Principal limitations and confounds of Experiment 1.

Issue	Implication
Edited-excerpt analysis	The supplied analytical sequence contains representative excerpts from longer repeated runs. Formal repeatability statistics require the complete uncut source recordings.

Issue	Implication
No randomized stimulus order	The bīja sequence was not described as randomized; time-dependent drift in water temperature, transducer state, or fluid condition therefore remains a possible confound even though the apparatus was unchanged.
Circular boundary	A circular bowl strongly constrains allowable modes and makes circular/annular geometry non-specific.
Uncharacterized acoustic spectra	The report does not yet include fundamental-frequency, harmonic-spectrum, SPL, or spectral-flux measurements for each bīja stimulus.
No independent apparatus replication	All results arise from one physical system. Reproduction with a second bowl/transducer geometry is required.
Exploratory analysis	The analysis pipeline and hypotheses evolved while viewing the data, particularly the move from whole-frame to radial-layer analysis. A preregistered/blinded replication is required for confirmatory inference.
Centre/radius sensitivity	Rotational Fourier estimates depend on the selected image centre and radial sampling range. Sensitivity analyses should perturb these parameters.
Harmonic ambiguity	A visible 8-fold parent can contribute 16-fold harmonics; a 3-fold form can coexist with 6-fold organization. Parent/harmonic relationships must be distinguished from independent 'petal' counts.
Lighting/optical edge effects	Gradient-based analysis measures visible image structure, which can be influenced by reflections and illumination as well as the water surface itself.
Layered OM is a modified stimulus	The strong Ājñā/2 result belongs to an OM + octave-down composite and cannot be treated as equivalent to unmodified OM.

10. Confirmatory programme arising from Experiment 1

The appropriate next phase is not to add further symbolic interpretations to the current excerpts. It is to convert the strongest exploratory findings into preregistered tests.

10.1 Full-run repeatability analysis

- Analyse every repetition in the original long LAM, VAM, RAM, YAM, HAM, and OM recordings.
- Estimate within-bīja recurrence of the predefined target architectures: LAM/4; VAM/6; RAM 3/6 + 10; YAM 6 + 12; HAM 8/16; OM/2 where relevant.
- Quantify transition time into each stable pattern family and pattern duration.
- Measure frame-to-frame and repetition-to-repetition similarity using correlation/SSIM plus rotational-spectrum similarity.

10.2 Blinded / preregistered classification

- Freeze the image-analysis pipeline before analysing a new dataset.
- Mask stimulus labels during image analysis.
- Predefine radial ranges, expected orders, scoring rules, exclusion windows, and primary endpoints.
- Test whether an algorithm can classify bīja identity above chance from rotational-spectrum features without access to labels.

10.3 Acoustic decomposition

- Measure fundamental frequency, formants, harmonic spectral envelope, RMS level, temporal modulation, and spectral flux for every stimulus.
- Pitch-shift individual bījas while preserving phonetic content to separate phoneme-dependent from pitch-dependent structure.
- Compare original, octave-down, and layered versions for each bīja, motivated by the strong change observed in the layered-OM Ājñā probe.

10.4 Apparatus controls

- Repeat at multiple water volumes/depths.
- Repeat in a second bowl diameter and shape.
- Repeat at controlled playback levels.
- Include sustained non-bīja vowels/tones and acoustically matched controls.
- Repeat in an independent laboratory if the initial findings survive internal replication.

11. Conclusion

Experiment 1 provides a substantive hypothesis-generating dataset linking traditional chakra bīja stimuli with measurable, layered rotational organization in a fixed water-cymatics system. The strongest direct correspondences are LAM/4, HAM/16, and the central twofold organization of the octave-layered OM Ājñā probe. RAM and YAM are more complex: their expected petal orders are weak as whole-field averages but become meaningful when the image is decomposed by radius and interpreted together with traditional parent geometries. The final unmodified OM/Sahasrāra observation contributes a different form of correspondence: dense multi-order radial multiplicity and subdivision, organized around a persistent 4/8/16/24 hierarchy, together with exceptionally strong empirical repeatability. This layered result is scientifically more interesting than a simple visual resemblance claim because it generates specific, falsifiable predictions for repeated and blinded experiments.

The central working hypothesis emerging from this record is that bīja-driven cymatic fields may contain characteristic rotational orders at different spatial scales, while the unmodified OM/Sahasrāra field may be characterized by the degree of simultaneous radial multiplicity and subdivision rather than by one literal petal number. Some of these measured architectures show nontrivial correspondence with numerical/geometric structures preserved in the traditional chakra model. The present evidence is not sufficient for causal or metaphysical conclusions. It is sufficient to justify a rigorous confirmatory research programme.

12. Reproducibility record

12.1 Files analysed

Table 9. Source video files used in this analytical record.

File	Role
chakra-test.mp4	Primary 67 s combined sequence
om-ajna.mp4	Layered OM Ājñā probe
new-ram-chakras.mp4	Auxiliary RAM exploratory recording

12.2 Analysis artefacts retained

Table 10. Figures and derived analytical artefacts embedded in this report.

Artefact	Description / key
chakra_symmetry_specificity.png	spec
lam_vam_ham_expected_order_candidates.jpg	lvh_candidates
lam_vam_ham_radial_profiles.png	lvh_radial
ram_triangle_10_candidates.jpg	ram_candidates
ram_3_6_10_radial_profile.png	ram_radial
yam_nested_6_12_candidates.jpg	yam_candidates
yam_6_12_radial_profile.png	yam_radial
om_ajna_2fold_candidates.jpg	om_candidates
om_ajna_radial_hierarchy.png	om_radial
om_ajna_time_hierarchy.png	om_time
first_ram_10_candidates.jpg	first_ram
ram_10_candidates.jpg	new_ram
figure_timeline.png	segment timeline
figure_expected_order_baseline.png	expected-order baseline
figure_correspondence_map.png	correspondence map
figure_analysis_workflow.png	analysis workflow
om_sahasrara_mean_spectra.png	Sahasrāra multi-order spectrum
om_sahasrara_radial_hierarchy.png	Sahasrāra radial hierarchy
om_sahasrara_highorder_heatmap.png	Sahasrāra high-order multiplicity
om_sahasrara_repeatability_frames.jpg	Sahasrāra repeatability validation frames

References

1. Woodroffe, J. G. (Arthur Avalon). (1919). The Serpent Power: Being the Ṣaṭ-Cakra-Nirūpaṇa and Pādukā-Pañcaka, Two Works on Tantrik Yoga. London: Luzac & Co.

2. Misseroni, D., Colquitt, D. J., Movchan, A. B., Movchan, N. V., & Jones, I. S. (2016). Cymatics for the cloaking of flexural vibrations in a structured plate. Scientific Reports, 6, 23929. https://doi.org/10.1038/srep23929

3. Escaler, X., & De La Torre, O. (2018). Axisymmetric vibrations of a circular Chladni plate in air and fully submerged in water. Journal of Fluids and Structures, 82, 432–445. https://doi.org/10.1016/j.jfluidstructs.2018.07.017

4. Crowther, R. A., & Amos, L. A. (1971). Harmonic analysis of electron microscope images with rotational symmetry. Journal of Molecular Biology, 60(1), 123–130. https://doi.org/10.1016/0022-2836(71)90452-9

5. Background historical descriptions of chakra petal counts and internal mandalas were checked against the 1919 Woodroffe/Avalon text and an online transcription of related material at the Internet Sacred Text Archive. The scientific interpretation in this report does not depend on treating these historical descriptions as empirical anatomy.

Appendix A. Key numerical observations retained from the exploratory analysis

Table A1. Compact numerical summary for future replication planning.

Stimulus	Target order	Key retained observations
LAM	4	Whole-section mean 0.331; top-3 97.56%; median rank 2; best-annulus mean ~0.560; ~1.71× enrichment
VAM	6	Whole-section mean 0.232; top-3 28.57%; median rank 6; best-annulus mean ~0.378; clear 9.6–11.4 s sixfold phase
RAM	10	Whole-section mean 0.139; top-3 2.22%; median rank 12; local 10-fold layer ~0.5–0.66; repeated 3/6 parent structure
YAM	12	Whole-section mean 0.135; global top-3 0%; median rank 16; local 12 reaches rank 1–3 at selected radii; nested 6/12 window ~34.4–35.1 s
HAM	16	Whole-section mean 0.172; top-3 45.65%; median rank 6.5; best-annulus mean ~0.316; ~1.31× enrichment; 8→16 hierarchy
Ājñā probe	2	Layered OM: 2-fold rank 1 in ~46% of sampled frames; top-3 in ~90%; median rank ~2; strongest centrally
OM / Sahasrāra	Multiplicity	Persistent 4/8/16/24 hierarchy; ~11 materially expressed rotational orders on average; repeated-presentation spectrum correlation ~0.997; strong radial subdivision

Appendix B. Interpretive hierarchy

For future public or scientific communication, the following hierarchy should be preserved:

- Observation: a measured rotational order is present at a defined time and radius.
- Pattern-level result: that order is persistent, dominant, enriched, or nested with another order.
- Traditional parallel: the measured architecture resembles a predefined numerical/geometric structure from the chakra model.
- Interpretation: the parallel may be meaningful and merits replication.

- Claim not supported by Experiment 1: that the chakra system has been scientifically proven, that ancient authors derived the diagrams from cymatics, or that the observed water geometry demonstrates a biological chakra mechanism.